Eburicoic acid inhibits endothelial cell pyroptosis and retards the development of atherosclerosis through the Keap1/Nrf2/HO-1/ROS pathway

MENG-QING MA[1], CHUN YANG[1], SHI-YU JIN[1], YU YANG[1], YAN-YAN PAN[2] and XIAN-HE LIN[1]

[1]Department of Cardiology, The First Affiliated Hospital of Anhui Medical University, Hefei, Anhui 230022, P.R. China; [2]Department of Cardiology, Hefei Cancer Hospital, Chinese Academy of Sciences, Hefei, Anhui 230022, P.R. China

Received October 6, 2024; Accepted March 12, 2025

DOI: 10.3892/mmr.2025.13551

Abstract. Atherosclerosis (AS)-related coronary artery disease is the main cause of morbidity and mortality around the globe. Eburicoic acid, a triterpenoid compound from *Antrodia camphorata*, exerts anti-inflammatory and anti-hyperlipidemic effects, although its role in atherogenesis remains unknown. Endothelial cell pyroptosis-caused chronic inflammatory response within vessel walls is a critical initial event in atherogenesis, making it a promising target to prevent AS. The present study was designed to investigate the effects of eburicoic acid on endothelial cell pyroptosis, AS progression and the underlying mechanisms. The results showed that with dose and time increased, treatment of human umbilical vascular endothelial cells (HUVECs) with eburicoic acid markedly decreased the expression of Kelch-like ECH-associated protein 1 (Keap1), NF-E2-related factor 2 (Nrf2), reactive oxygen species (ROS), NLR family pyrin domain-containing protein 3 (NLRP3), cleaved caspase-1, apoptosis-associated speck-like protein containing CARD (ASC), N-terminal gasdermin-D (GSDMD-N), downregulated the secretion levels of pro-inflammatory cytokines interleukin (IL) 1β, IL-6 and IL-18, inhibited caspase-1 activity and lactate dehydrogenase release and improved plasma membrane integrity. By contrast, the expression of nuclear Nrf2, total Nrf2 and heme oxygenase-1 (HO-1) were increased by eburicoic acid treatment in HUVECs dose- and time-dependently. Moreover, the inhibitory effects of eburicoic acid on HUVEC pyroptosis were mainly compromised by pre-treatment with ROS agonist, HO-1 small interfering (si)RNA, or Nrf2 siRNA. Finally, it was observed that administering high-fat-diet fed ApoE$^{-/-}$ mice with eburicoic acid markedly increased Nrf2 and HO-1 levels and reduced the expression of Keap1, NLRP3, cleaved caspase-1, ASC and GSDMD-N in aortas and ameliorated hyperlipidemia and inflammation in the serum, leading to smaller atherosclerotic plaques, less lipid accumulation and high content of collagen fiber within plaques. These findings identified eburicoic acid as a potent anti-atherogenic natural product by suppressing endothelial cell pyroptosis via the Keap1/Nrf2/HO-1/ROS pathway. Eburicoic acid may be considered an effective phytomedicine for treating AS.

Correspondence to: Professor Xian-He Lin, Department of Cardiology, The First Affiliated Hospital of Anhui Medical University, 218 Jixi Road, Shushan, Hefei, Anhui 230022, P.R. China
E-mail: xianhelin2001@163.com

Key words: eburicoic acid, nuclear factor erythroid 2-related factor 2, heme oxygenase-1, endothelial cell pyroptosis, atherosclerosis

Introduction

Coronary heart diseases (CADs) and their various complications, including cardiomegaly, angina pectoris and myocardial infarction, are the proegumenal cause of human morbidity and mortality worldwide (1). Atherosclerosis (AS) is the pathological foundation of various CADs. AS-induced coronary artery stenosis and insufficient blood flow to the myocardium lead to cardiomyocyte ischemia and a dysfunctional heart (2). Chronic endothelial inflammation in the aorta is a crucial trigger for atherosclerotic plaque formation (3). Endothelial BTB and CNC homology 1 deficiency could decrease the expression of intercellular cell adhesion molecule-1 (ICAM-1) and vascular cell adhesion molecule-1(VCAM-1), reduce plasma tumor necrosis factor-α (TNF-α) and interleukin (IL)1β levels, ameliorating turbulent blood flow- or high-fat-diet (HFD)-induced plaque formation in atherosclerotic mice (4). In gonadotropin-releasing hormone agonist-treated mice, blockade of follicle-stimulating hormone decreases VCAM-1 levels and mitigates endothelial inflammation, causing smaller atherosclerotic lesions with increased plaque stabilities (5). Pyroptosis, a pro-inflammatory form of programmed cell death, is crucial in amplifying protective immunity against pathogen invasion (6). It is characterized by activating inflammatory caspases (caspase-1/4/15) and gasdermin (GSDM), causing cell swelling, pore formation of plasma membranes and the robust release of IL-1β, IL-18 and high-mobility group box 1 (7). Vascular endothelial cells (VECs) line the inner surface of vessel walls. The injury and abnormal death of VECs may decrease nitric oxide (NO) production, amplify adhesion molecule expression and inflammation and induce dysfunctional

angiogenesis, leading to accelerated AS and a higher risk of cardiovascular events (8). Yin *et al* (9) observed that in apoE$^{-/-}$ mice fed an HFD for 3 weeks, the activity of caspase-1 in VECs was markedly increased. In caspase-1-deficient ApoE$^{-/-}$ mice, endothelial activation, vascular inflammation and the size of atheromatous plaques were decreased considerably. Low-shear stress (LSS) can induce VEC pyroptosis *in vitro* and *in vivo* and promote the development of AS through the IKKε/STAT1/NLRP3 pathway (10). Trimethylamine N-oxide (TMAO), a well-known pro-atherogenic factor, could upregulate phosphatidylethanolamine acyltransferase and induce excessive mitophagy, leading to human umbilical vein endothelial cell (HUVEC) pyroptosis and inflammation (11). These recent findings denote the critical negative role of VEC inflammation and pyroptosis in atherogenesis.

Compared with western medicine, Chinese herbal medicines have enormous advantages in improving the environment of the immune system to gain long-lasting effects and prevent potential adverse effects (12). Chinese herbal medicines and active metabolites, such as resveratrol (13), curcumin (14), salidroside (15), quercetin (16) and berberine (17), possess multiple anti-atherogenic activities. Eburicoic acid (Fig. 1A) is a triterpenoid derivative extracted from the fruiting bodies of *Antrodia cinnamomea*. It is also an active ingredient from Banxia Baizhu Tianma Decoction, a Chinese herbal formula widely used to treat CADs. So far, research regarding the biological effects of eburicoic acid in various diseases is still preliminary. Deng *et al* (18) injected ICR mice with λ-carrageenan (Carr), a seaweed polysaccharide, to induce the paw edema model. They found that Carr-induced increase in serum levels of TNF-α and IL-1β was markedly inhibited following the administration of eburicoic acid. Tung *et al* (19) found that compared with normoxic mice, treating hyperoxia mice with eburicoic acid decreases NF-κB, IL-6, TNF-α, IL-1β and IL-8 levels in lung tissue. Su *et al* (20) observed that treating human hepatoma cells with eburicoic acid effectively decreases cell viability by inducing endoplasmic reticulum stress-mediated autophagy and reactive oxygen species (ROS) production. Intraperitoneal injection of eburicoic acid into CCL4-treated mice decreases hepatic levels of inducible nitric oxide synthase (iNOS) and cyclooxygenase-2 (COX2) and increased the activities of several antioxidant enzymes (21). Wang *et al* (22) reported that incubation of RAW264.7 macrophages with eburicoic acid decreases the production of NO, iNOS, prostaglandin E2 (PGE2) and COX2 and downregulates the secretion level of pro-inflammatory cytokines, including TNF-α, IL-6 and IL-1β, by inhibiting the activation of PI3K/Akt/mTOR/NF-κB pathways. Moreover, administering HFD-fed mice with eburicoic acid markedly decreases blood glucose, triglycerides (TG) and total cholesterol (TC) levels, ameliorating adipocyte hypertrophy and hepatocytic ballooning (23). These findings reveal that eburicoic acid exerts anti-inflammatory, anti-hyperlipidemic and anti-diabetic effects and may protect against AS. The present study was designed to investigate the effect of eburicoic acid on VEC pyroptosis and atherogenesis, as well as the underlying mechanisms, aiming at identifying eburicoic acid as a novel phytomedicine in treating AS.

Materials and methods

Cell culture. HUVECs (ATCC; cat. no. CRL-1730) were cultured in RPMI 1640 medium (Gibco; Thermo Fisher Scientific, Inc.; cat. no. 11875093) containing 10% FBS (Procell Life Science & Technology Co., Ltd.; cat. no. 164210), 20 μg/ml penicillin and 20 μg/ml streptomycin. Cells were maintained in an incubator under a humidified atmosphere of 5% CO_2 and 95% air at 37˚C. They were seeded in 6- or 96-well plates with serum-free RPMI 1640 medium for at least 6 h to obtain the synchronization of growth before the experiments commenced. Prior to other treatments, cells were treated with 100 μg/ml oxidized low-density lipoprotein (ox-LDL) (Yiyuan Biotechnology Co., Ltd.; cat. no. YB-002) for 24 h to induce pyroptosis. Besides, cells were pre-incubated with 10 μM DMNQ (ROS agonist; MedChemExpress; cat. no. HY-121026) for 6 h to increase ROS production.

Small interfering RNA (siRNA) transfection. siRNA targeting HO-1 (NCBI Gene ID: 3162), NF-E2-related factor 2 (Nrf2; NCBI Gene ID: 4780) and scrambled control siRNA were designed and synthesized by Shanghai GenePharma Co., Ltd. using GenePharma RNAi designer V2.0 software. Prior to transfection, cells were planted in 6-well plates (2x10^6/well) and cultured in RPMI 1640 medium without FBS or antibiotics for 12 h. siRNA-Lipofectamine® 2000 (Invitrogen; Thermo Fisher Scientific, Inc.) transfection mixture, including 125 μl Opti-MEM® Medium (Gibco; Thermo Fisher Scientific, Inc.; cat. no. 31985-062), 100 pmol (5 μl) siRNA and 5 μl Lipofectamine® 2000 reagent (Thermo Fisher; cat. no. 11668019) for 48 h at 37˚C. Western blotting was used to evaluate the transfection efficiency. The siRNA sequences were as follows: HO-1 siRNA, 5'-GGGUGAUAGAAGAGG CCAATT-3'; Nrf2 siRNA, 5'-CUAUCACUUUGCAAAGCU UUCAACC-3'; scrambled control siRNA, 5'-UUCUCCGAA CGUGUCACGUTT-3'.

Reverse transcription-quantitative (RT-q) PCR. After HUVECs (2x10^6/well) were subjected to different treatments, the total RNAs were extracted using the TRIzol® reagent (Thermo Fisher Scientific, Inc.; cat. no. 15596018) according to the manufacturer's protocol. A Nanodrop 3000 spectrophotometer (Thermo Fisher Scientific, Inc.) was used to detect the purity of obtained RNAs. Genomic DNA (gDNA) elimination and cDNA synthesis are performed using the PrimeScript RT Reagent Kit (Takara Biotechnology Co., Ltd.; cat. no. RR047A). Briefly, 1 μg total RNA was transferred to a 0.2 ml EP tube, dissolved in 7 μl RNase-Free dH_2O, followed by incubation with 1 gDNA Eraser and 2 μl 5XgDNA Eraser Buffer to remove contaminating gDNA. Then, the EP tube was added with 4 μl 5x PrimeScript Buffer 2, 1 μl PrimeScript RT Enzyme Mix1, 1 μl RT Primer Mix and 4 μl RNase Free dH_2O at 37˚C for 15 min. This reaction was ended at 85˚C for 5 sec and cDNA was obtained. The cDNA was then subjected to PCR amplification using TB Green® Premix Ex Taq™ II (Takara Biotechnology Co., Ltd.; cat. no. RR820A) on an ABI 7500 Fast Real-Time PCR System (Applied Biosystems; Thermo Fisher Scientific, Inc.) to detect the expression of target genes, including Nrf2, HO-1, NLRP3, ASC, caspase-1 and GSDMD. The PCR reaction mixture involved 2 μl cDNA,

10 μl TB Green Premix Ex Taq II (2X), 0.8 μl forward primer (10 μM), 0.8 μl reverse primer (10 μM), 0.4 μl ROX Reference Dye II (50X) and 6 μl dH_2O. The PCR conditions were 30 sec at 95˚C for pre-denaturation, 40 cycles of 5 sec at 95˚C and 30 sec at 60˚C. Sangon Biotech Co., Ltd. designed and synthesized all primers, the sequences of which are listed in Table SI. The relative expression of target genes was evaluated using the $2^{-\Delta\Delta Cq}$ method (24) and the GAPDH level was used as an internal control. The PCR reactions were repeated three times from three independent experiments.

Western blotting. After the different treatments of HUVECs and apoE$^{-/-}$ mice, cells and aortic tissues were harvested and the proteins were extracted using the mixture of RIPA buffer (Beijing Solarbio Science & Technology Co., Ltd.; cat. no. R0010), 1% PMSF (Beijing Solarbio Science & Technology Co., Ltd.; cat. no. P0100) and 1% protein phosphatase inhibitor (Beijing Solarbio Science & Technology Co., Ltd.; cat. no. P1260). The lysate solutions were transferred into a 1.5 ml EP tube and centrifuged at 12,000 g for 5 min at 4˚C. The supernatants were carefully collected and 10 μl of the solution was used to quantify protein concentrations using a BCA assay kit (Beijing Solarbio Science & Technology Co., Ltd.; cat. no. PC0020). The rest of the protein solutions were mixed with an SDS-loading buffer (5X) at a ratio of 1:4 and boiled for 10 min for denaturation. The nuclear and cytoplasmic proteins were extracted according to the instructions of the nuclear and cytoplasmic protein extraction kit (Wuhan Boster Biological Technology, Ltd.; cat. no. AR0106). Equal amounts of protein were loaded onto 10% SDS-PAGE (~15 μl/lane) fractionated by SDS-PAGE at a constant voltage of 110 V for 1.5 h, followed by transfer into the 0.45 μm PVDF membranes (260 mA, 2 h). The membranes were probed with primary antibodies (1:1,000) against Kelch-like ECH-associated protein-1 (Keap1; Proteintech Group, Inc.; cat. no. 10503-2-AP), Nrf2 (Proteintech Group, Inc.; cat. no. 80593-1-RR), HO-1 (Proteintech Group, Inc.; cat. no. 81281-1-RR), NLRP3 (Proteintech Group, Inc.; cat. no. 27458-1-AP), ASC (Proteintech Group, Inc.; cat. no. 10500-1-AP), caspase-1 (Proteintech Group, Inc.; cat. no. 22915-1-AP), caspase-3 (Proteintech Group, Inc.; cat. no. 82202-1-RR), caspase-8 (Proteintech Group, Inc.; cat. no. 13423-1-AP), Bcl-2 (Proteintech Group, Inc.; cat. no. 12789-1-AP), Bax (Proteintech Group, Inc.; cat. no. 50599-2-Ig), glutathione peroxidase 4 (GPX4; Proteintech Group, Inc.; cat. no. 30388-1-AP), SLC7A11 (Proteintech Group, Inc.; cat. no. 26864-1-AP), FPN (Proteintech Group, Inc.; cat. no. 26601-1-AP), ACSL4 (Proteintech Group, Inc.; cat. no. 22401-1-AP), TLR4 (Proteintech Group, Inc.; cat. no. 19811-1-AP), GAPDH (Proteintech Group, Inc.; cat. no. 10494-1-AP) and lamin B1 (Proteintech Group, Inc.; cat. no. 12987-1-AP) overnight at 4˚C with gentle shaking. Skimmed milk powder (5%) in TBS-T buffer (0.05% Tween-20) diluted the antibodies. Afterwards, immunoblotted membranes were rinsed in TBS-T solution (three times, 10 min/time) and incubated with HRP-conjugated secondary antibodies (1:5,000, Proteintech Group, Inc.; cat. no. 10500-1-AP) for 4 h at 4˚C. Following rinsed triple times in TBS-T, membranes were dried and subjected to visualize gel blots using the Immobilon® ECL UltraPlus Western HRP Substrate (Merck KGaA; cat. no. WBULP-10ML). Image Pro Plus software 7.0 (Media Cybernetics, Inc.) was used to assess the density of protein bands and analyze the relative protein expression. GAPDH was used as the internal standard for total and cytoplasmic proteins and lamin B1 was used as the loading control for nuclear proteins.

ELISA assay. After the different treatments of HUVECs and apoE$^{-/-}$ mice, the culture medium and serum samples were collected to evaluate the secretion of pro-inflammatory cytokines. The levels of human IL-1β (Wuhan Boster Biological Technology, Ltd.; cat. no. EK0392), mouse IL-1β (Wuhan Boster Biological Technology, Ltd.; cat. no. EK0394), human IL-6 (Wuhan Boster Biological Technology, Ltd.; cat. no. EK0410), mouse IL-6 (Wuhan Boster Biological Technology, Ltd.; cat. no. EK0411), human IL-18 (Wuhan Boster Biological Technology, Ltd.; cat. no. EK0864), mouse IL-18 (Wuhan Boster Biological Technology, Ltd.; cat. no. EK0433) and mouse TNF-α (Wuhan Boster Biological Technology, Ltd.; cat. no. EK0527) were measured by corresponding commercial ELISA kits per the manufacturer's instructions. Absorbance at 450 nm was monitored using an iMark Microplate Absorbance Reader (Bio-Rad Laboratories, Inc.).

Caspase-1 activity assay. Caspase-1 activity was assessed according to the manual instructions within the caspase-1 activity assay kit (Beyotime Institute of Biotechnology; cat. no. C1101). Cells were seeded into 6-well plates at a density of 2x10^6/well. When cells were 70-80% confluent, they were treated or transfected with different agents. Afterward, the mediums were removed and lysis buffer was added into each well (200 μl/well) for 30 min at 4˚C. Cell debris was collected, transferred into a 1 ml EP tube and centrifuged at 12,000 g for 5 min at 4˚C. The supernatants were harvested and protein concentrations were determined using a BCA assay. The EP tube was then supplemented with 10 μl AcYVAD-pNA for 2 h at 37˚C. Absorbance at 405 nm was recorded and the standard pNA (yellow) curve was drawn to evaluate the caspase-1 activity. Data were presented as fold change normalized to control.

Lactate dehydrogenase (LDH) release assay. LDH release assay was applied to evaluate plasma membrane damage using an LDH cytotoxicity assay kit (Beyotime Institute of Biotechnology; cat. no. C0016). After treatment or transfection, HUVECs were planted in 96-well plates (1x10^4/well) with 100 μl RPMI complete medium. Each well was added with 10 μl LDH release solution and cultured in a humidified 5% CO_2 incubator for 12 h. Through lysis and centrifugation at 12,000 g for 5 min at 4˚C, an aliquot of 50 μl medium or cell lysates was mixed with 60 μl LDH working solution, including 20 μl 1X INT solution, 20 μl enzyme solution and 20 μl lactic acid solution, for 30 min at 4˚C in the dark. Absorbance at 490 nm was monitored using a microplate spectrophotometer. The percentage of LDH release was calculated as the absorbance of the supernatant divided by the absorbance of the supernatant plus the absorbance of the lysate, as previously described (25).

Hoechst/PI staining assay. Hoechst 33342/PI double staining assay detected plasma membrane integrity. HUVECs were seeded in 6-well plates and treated differently. Cells were washed with PBS twice and the remaining medium was removed entirely. Following the manual instructions (Beijing Solarbio Science & Technology Co., Ltd.; cat. no. CA1120), each well was supplemented with 1 ml staining buffer, 5 μl Hoechst solution and 5 μl PI solution with a gentle shake. The plate was then incubated at 4˚C for 30 min in the dark. After rinsing in PBS, the staining solution was disposed of and the images were captured using a fluorescent microscope.

Determination of intracellular ROS levels. Per the manufacturer's guidance, cellular ROS content was measured using a ROS assay kit (Beyotime Institute of Biotechnology; cat. no. S0033M). Briefly, fluorescent probe DCFH-DA was diluted into 10 μM using serum-free RPMI medium and stored in the dark. HUVECs were seeded in 6-well plates ($2x10^6$/well) and treated differently, followed by incubation with 10 μM DCFH-DA (1 ml/well) at 37˚C for 20 min in the humidified 5% CO_2 incubator. Then, each well was rinsed with cold PBS triple times to remove redundant probes. Representative images were taken with a fluorescent microscope.

Animal treatment. A total of 30 8-week-old male $apoE^{-/-}$ mice on C57BL/6J background were bought from Nanjing Junke Bioengineering Co., Ltd. Mice were housed at 24±2˚C and 50±5% humidity on a 12-h light/dark cycle with free access to water and food. All mice were fed a high-fat diet (HFD; 21% fat, 0.3% cholesterol) and randomized into the control and eburicoic acid groups (n=15/group). Mice in the eburicoic acid group were administered 10 mg/kg eburicoic acid (MedChemExpress; cat. no. HY-122951), dissolved in 0.5% carboxymethyl cellulose (CMV) daily by oral gavage. The control group was orally treated with an equivalent amount of 0.5% CMV daily. At 12 weeks, mice were anesthetized using 3% pentobarbital sodium (30 mg/kg, i.p.), euthanized by cervical dislocation and dissected. The hearts, aortas and blood were collected for further analysis. The Anhui Medical University Ethics Committee approved all animal procedures (approval no. LLSC20242407) per the Declaration of Helsinki.

Evaluation of atherosclerotic plaques in the aortic roots. Freshly isolated hearts were rinsed in PBS, fixed in 4% paraformaldehyde at 4˚C overnight and embedded in OCT compound (Sakura Finetek USA, Inc.; cat. no. 4583) at -20˚C overnight. Serial 6-μm-thick cryosections were obtained throughout the three aortic valves (eight sections/mouse). They were stained with Oil Red O (Beijing Solarbio Science & Technology Co., Ltd.; cat. no. G1261), hematoxylin and eosin (H&E, Beijing Solarbio Science & Technology Co., Ltd.; cat. no. G1120) and Masson (Beijing Solarbio Science & Technology Co., Ltd.; cat. no. G1346) for 30 min at 37˚C to detect lipidosis, plaque area and collagen contents. Representative images were captured using an inverted microscope (IX-81; Olympus Corporation). The positive-staining area was calculated using Image Pro Plus software 7.0 (Media Cybernetics, Inc.) and normalized to the cross-sectional luminal area.

Detection of serum levels of lipids, pro-inflammatory cytokines and biochemical indices. Prior to sacrifice, blood samples (~1.5 ml/mouse) were obtained from the retro-orbital plexus under anesthesia and kept in EDTA-coated tubes. After centrifugation at 5,000 g at 4˚C for 10 min, the supernatants (serum) were gathered into another EP tube, followed by the detection of aspartate aminotransferase (AST; cat. no. C010-2-1), alanine aminotransferase (ALT; cat. no. C009-2-1), blood urea nitrogen (BUN; cat. no. C013-2-1), TC (cat. no. A111-1-1), low-density lipoprotein cholesterol (LDL-C; cat. no. A113-1-1), high-density lipoprotein protein cholesterol (HDL-C; cat. no. A112-1-1) and TG (cat. no. A110-1-1) following the manufactural instructions in the commercial kits (Nanjing Jiancheng Bioengineering Institute). The serum levels of IL-1β, IL-6, IL-18 and TNF-α were detected using ELISA, as aforementioned.

Statistical analyses. All experiments were repeated at least three independent times. Data were processed using GraphPad Prism 10.1 software (Dotmatics) and analyzed using unpaired Student's t-test or one-way ANOVA followed by Tukey's test. Results were expressed as the mean ± standard deviation (SD). $P<0.05$ was considered to indicate a statistically significant difference.

Results

Eburicoic acid inhibits ox-LDL-induced NLRP3 inflammasome activation and pyroptosis in HUVECs in a dose- and time-dependent manner. The present study detected the effects of eburicoic acid on pyroptosis and inflammation in HUVECs induced by ox-LDL. HUVECs were maintained in a fresh serum-free medium for 6 h for synchronization and treated with 100 μg/ml ox-LDL for 24 h. Then, cells were incubated with a fresh serum-free medium containing various concentrations of eburicoic acid (1, 5, 10 and 20 μg/ml) for 24 h. RT-qPCR and western blotting showed that with increasing dose, eburicoic acid markedly decreases pyroptosis-related factors' mRNA and protein levels, including NLRP3, ASC, cleaved caspase-1 and GSDMD-N (Fig. 1B and C). The secretion of pro-inflammatory cytokines (IL-1β, IL-6 and IL-18), caspase-1 activity and LDH release were reduced after eburicoic acid treatment (Fig. 1D-F). Hoechst/PI staining showed that eburicoic acid improved the plasma membrane integrity (Fig. 1G). These effects of eburicoic acid were observed even at a low concentration of 1 μg/ml, with the most substantial effect at 20 μg/ml. Then, HUVECs were treated with 10 μg/ml eburicoic acid for 6, 12, 24 and 48 h to investigate whether eburicoic acid can repress inflammation and pyroptosis time-dependently. The results showed that ox-LDL-induced pyroptosis indicator mRNA and protein expression, secretion of pro-inflammatory factors, caspase-1 activity, LDH release and plasma membrane disruption were inhibited in HUVECs after incubation with 10 μg/ml eburicoic acid for 6 h. These effects were more pronounced as the incubation time was prolonged, peaking at 48 h (Fig. 2). In the meantime, it was observed that eburicoic acid did not affect the expression of apoptosis- and ferroptosis-related proteins in

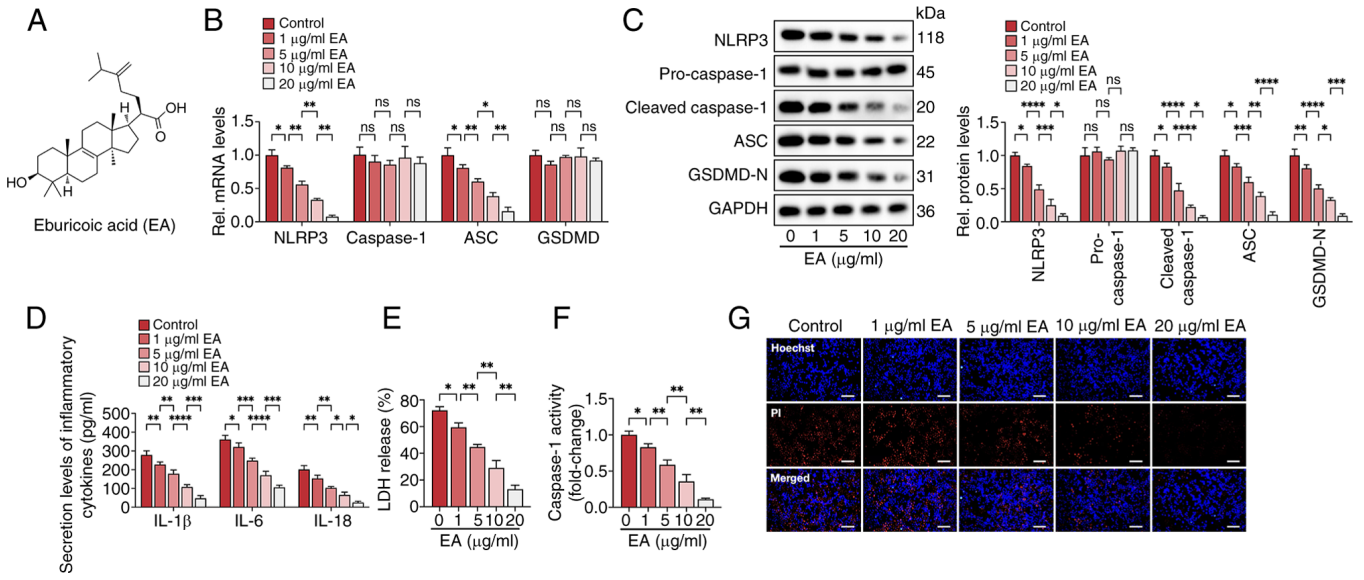

Figure 1. Eburicoic acid inhibits NLRP3 inflammasome activation and pyroptosis in ox-LDL-treated HUVECs in a dose-dependent manner. Cells were incubated with 100 μg/ml ox-LDL for 24 h, followed by treatment with 1, 5, 10 and 20 μg/ml eburicoic acid for 24 h. (A) Chemical structure of eburicoic acid; (B) RT-qPCR analyses of NLRP3, caspase-1, ASC and GSDMD mRNA levels. (C) western blotting analyses of NLRP3, pro-caspase-1, cleaved caspase-1, ASC and GSDMD-N protein levels; (D) ELISA Analyses of IL-1β, IL-6 and IL-18 secretion levels; (E) Determination of LDH release using an LDH release assay kit; (F) Spectrophotometry analysis of caspase-1 activity; (G) Representative images of Hoechst/PI staining. Data are represented as mean ± SD. ns, statistically insignificant, *P<0.05, **P<0.01, ***P<0.001, ****P<0.0001. Scale bar, 20 μm. n=3. EA, eburicoic acid; NLRP3, NLR family pyrin domain-containing protein 3; ox-LDL, oxidized low-density lipoprotein; HUVECs, human umbilical vascular endothelial cells; RT-qPCR, reverse transcription-quantitative PCR; ASC, apoptosis-associated speck-like protein containing CARD; GSDMD-N, N-terminal gasdermin-D; LDH, lactate dehydrogenase.

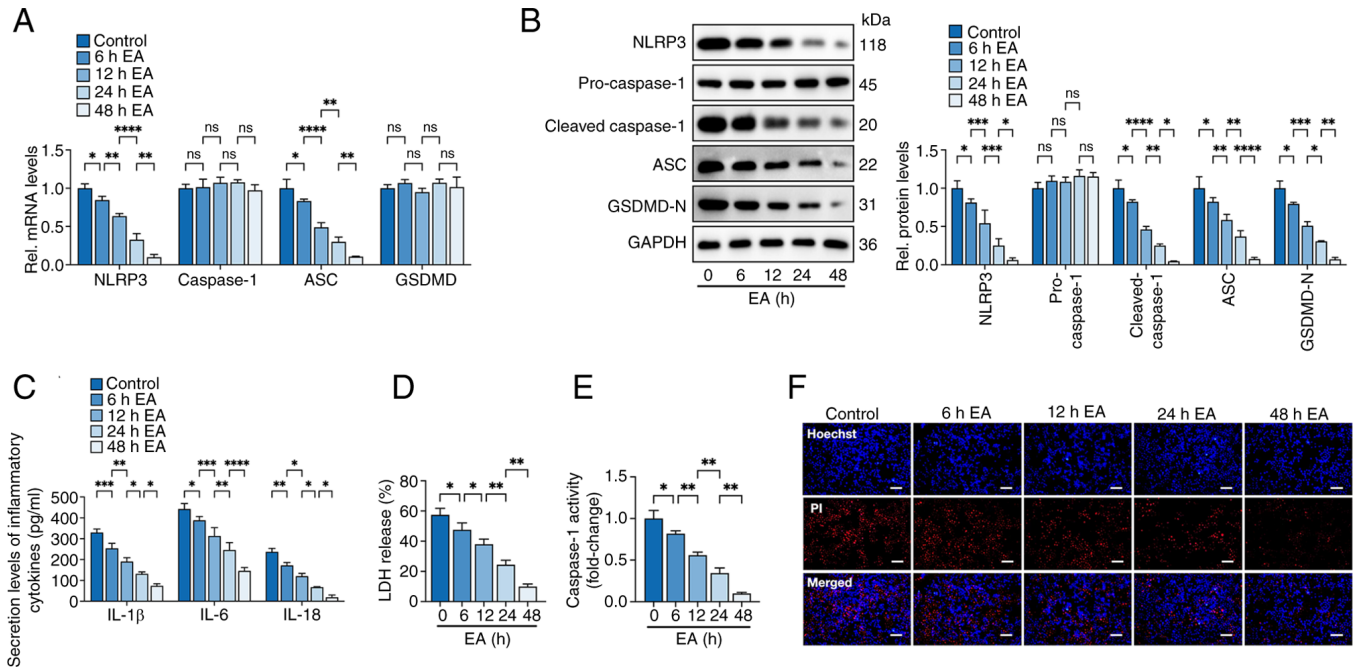

Figure 2. Eburicoic acid inhibits NLRP3 inflammasome activation and pyroptosis in ox-LDL-treated HUVECs in a time-dependent manner. Cells were incubated with 100 μg/ml ox-LDL for 24 h, followed by treatment with 10 μg/ml eburicoic acid. (A) RT-qPCR analyses of NLRP3, caspase-1, ASC and GSDMD mRNA levels; (B) western blotting analyses of NLRP3, pro-caspase-1, cleaved caspase-1, ASC and GSDMD-N protein levels; (C) ELISA Analyses of IL-1β, IL-6 and IL-18 secretion levels; (D) Determination of LDH release using an LDH release assay kit; (E) Spectrophotometry analysis of caspase-1 activity; (F) Representative images of Hoechst/PI staining. Data are represented as mean ± SD. ns, statistically insignificant, *P<0.05, **P<0.01, ***P<0.001, ****P<0.0001. Scale bar, 20 μm. n=3. NLRP3, NLR family pyrin domain-containing protein 3; ox-LDL, oxidized low-density lipoprotein; HUVECs, human umbilical vascular endothelial cells; RT-qPCR, reverse transcription-quantitative PCR; ASC, apoptosis-associated speck-like protein containing CARD; GSDMD-N, N-terminal gasdermin-D; IL, interleukin; LDH, lactate dehydrogenase EA, eburicoic acid.

ox-LDL-treated HUVECs (Figs. S1 and S2). These findings demonstrated that eburicoic acid inhibited ox-LDL-induced NLRP3 inflammasome activation and pyroptosis in a dose and time-dependent manner in HUVECs.

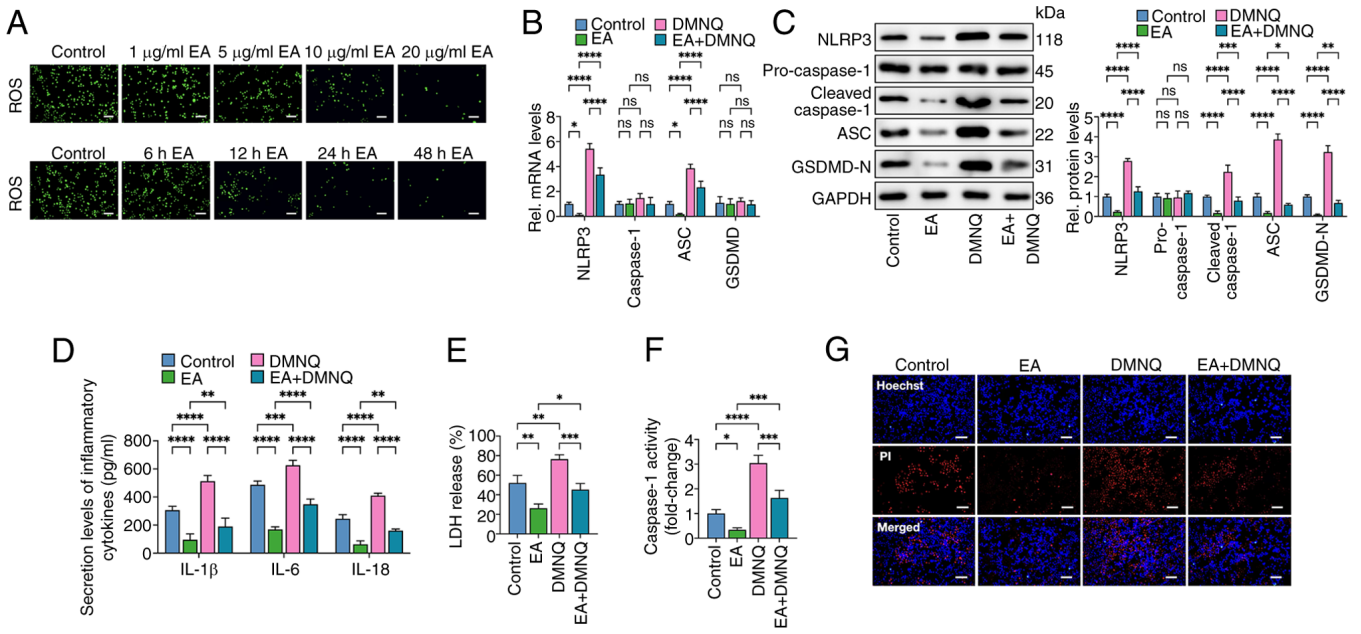

Figure 3. Eburicoic acid inhibits NLRP3 inflammasome activation and pyroptosis in ox-LDL-treated HUVECs by decreasing ROS production. (A) HUVECs were pre-treated with 100 μg/ml ox-LDL for 24 h and further incubated with 1, 5, 10 and 20 μg/ml eburicoic acid for 24 h or incubated with 10 μg/ml eburicoic acid for 6, 12, 24 and 48 h, respectively. Intracellular ROS production was detected using the peroxide-sensitive fluorescent probe DCFH-DA. (B-G) Cells were pre-treated with 100 μg/ml ox-LDL for 24 h. Then, cells were treated with 10 μg/ml eburicoic acid for 24 h, with or without co-incubation of 10 μM DMNQ (ROS agonist) for 6 h. (B) RT-qPCR analyses of NLRP3, caspase-1, ASC and GSDMD mRNA levels; (C) western blotting analyses of NLRP3, pro-caspase-1, cleaved caspase-1, ASC and GSDMD-N protein levels; (D) ELISA Analyses of IL-1β, IL-6 and IL-18 secretion levels; (E) Determination of LDH release using an LDH release assay kit; (F) Spectrophotometry analysis of caspase-1 activity; (G) Representative images of Hoechst/PI staining. Data are represented as mean ± SD. ns, statistically insignificant, *P<0.05, **P<0.01, ***P<0.001, ****P<0.0001. Scale bar, 20 μm. n=3. NLRP3, NLR family pyrin domain-containing protein 3; ox-LDL, oxidized low-density lipoprotein; HUVECs, human umbilical vascular endothelial cells; ROS, reactive oxygen species; RT-qPCR, reverse transcription-quantitative PCR; ASC, apoptosis-associated speck-like protein containing CARD; GSDMD-N, N-terminal gasdermin-D; IL, interleukin; LDH, lactate dehydrogenase EA, eburicoic acid.

Eburicoic acid inhibits ox-LDL-induced pyroptosis by decreasing ROS production in HUVECs. Previous studies have noted that ROS accumulation is closely related to NLRP3 inflammasome activation and pyroptosis (26,27). The present study explored whether eburicoic acid inhibited ox-LDL-induced macrophage pyroptosis by decreasing ROS. Cells were treated with 100 μg/ml ox-LDL for 24 h and incubated with various concentrations of eburicoic acid (1, 5, 10 and 20 μg/ml) for 24 h or 10 μg/ml for different durations (6, 12, 24 and 48 h). The results showed that eburicoic acid decreased ROS production dose- and time-dependently (Fig. 3A). Then, cells were treated with 10 μg/ml eburicoic acid for 24 h, with or without 10 μM DMNQ (ROS agonist) for 6 h. As reflected in Fig. 3B-G, the inhibitory effects of eburicoic acid on the expression of pyroptosis-related factors, secretion of pro-inflammatory factors, caspase-1 activity, LDH release and plasma membrane injury were mainly reversed, suggesting that eburicoic acid suppresses pyroptosis and inflammation by reducing ROS generation in ox-LDL-treated HUVECs.

Eburicoic acid inhibits ox-LDL-induced NLRP3 inflammasome activation and pyroptosis in HUVECs via the HO-1/ROS pathway. Heme oxygenase-1 (HO-1) is critical in inflammatory responses, oxidative stress, iron metabolism and vascular physiology. Increased HO-1 expression is associated with facilitated ROS removal and cellular redox balance maintenance (28,29). It was hypothesized that HO-1 was involved in the suppressive effects of eburicoic acid on ROS accumulation and pyroptosis of HUVECs. RT-qPCR and western blotting showed that eburicoic acid treatment markedly increased the mRNA and protein levels of HO-1 in a dose- and time-dependent manner (Fig. 4A-D). Then, cells were transfected with HO-1 siRNA to decrease HO-1 expression. As shown in Fig. 4E, the protein levels of HO-1 were diminished by nearly 85.4% following HO-1 siRNA treatment, indicating an effective transfection. Moreover, HO-1 silencing markedly reversed the repressive effects of eburicoic acid on ROS production, inflammation and pyroptosis in HUVECs (Fig. 4F-K). These observations suggested that eburicoic acid could suppress pyroptosis of HUVECs via the HO-1/ROS pathway.

Eburicoic acid ameliorates inflammation and pyroptosis in ox-LDL-treated HUVECs via the Keap1/Nrf2/HO-1/ROS pathway. Evidence has identified that HO-1 is a critical functional effector of Nrf2-induced ROS clearance and anti-oxidation. Under basal conditions, Nrf2 is mainly sequestered in the cytoplasm by binding to Kelch-like ECH-associated protein-1 (Keap1) (30). Under oxidative and electrophilic stress, Nrf2 is released from Keap1 and enters the nucleus, where Nrf2 binds to the antioxidant response element and promotes HO-1 expression (31,32). Next, the present study detected whether eburicoic acid promoted Nrf2 nuclear translocation in ox-LDL-treated HUVECs. Cells were treated with 100 μg/ml ox-LDL for 24 h, followed by incubation with various concentrations of eburicoic acid (1,5,10 and 20 μg/ml) for 24 h or 10 μg/ml for different durations (6, 12, 24 and 48 h). As shown in Fig. 5, eburicoic acid markedly decreased cytoplasmic Keap1 and Nrf2 protein levels dose- and time-dependently

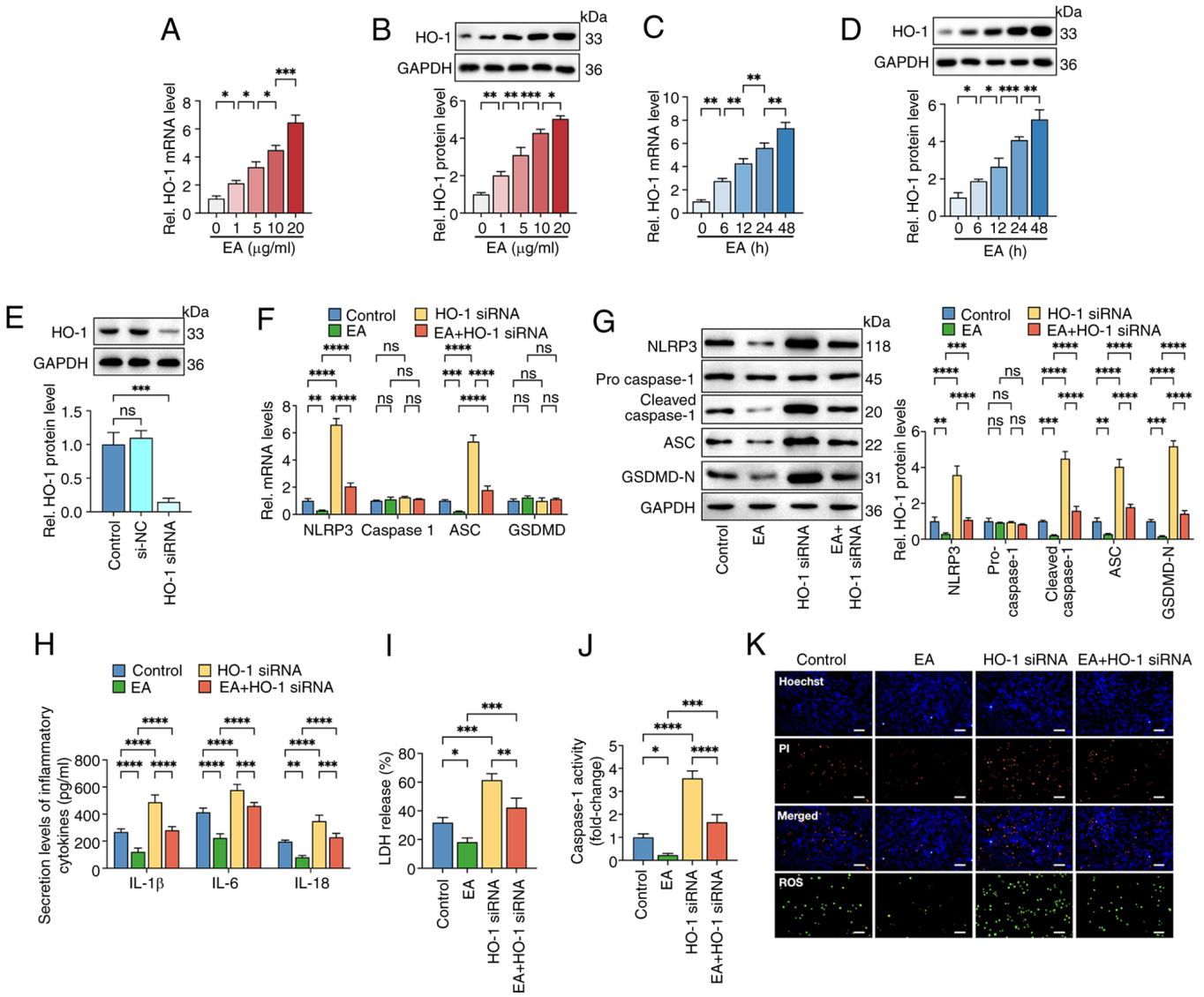

Figure 4. Eburicoic acid inhibits NLRP3 inflammasome activation and pyroptosis in ox-LDL-treated HUVECs via the HO-1/ROS pathway. HUVECs were pre-treated with 100 μg/ml ox-LDL for 24 h and further incubated with (A and B) 1, 5, 10 and 20 μg/ml eburicoic acid for 24 h or (C and D) incubated with 10 μg/ml eburicoic acid 6, 12, 24 and 48 h, respectively. The mRNA and protein levels of HO-1 were detected using RT-qPCR and western blotting, respectively. (E) Cells were transfected with HO-1 siRNA or scrambled control siRNA for 48 h. Western blotting was used to detect HO-1 protein level. Cells were pre-treated with 100 μg/ml ox-LDL for 24 h. Then, they were transfected with HO-1 siRNA for 48 h before treatment with 10 μg/ml eburicoic acid for 24 h. (F) RT-qPCR analyses of NLRP3, caspase-1, ASC and GSDMD mRNA levels. (G) Western blotting analyses of NLRP3, pro-caspase-1, cleaved caspase-1, ASC and GSDMD-N protein levels. (H) ELISA Analyses of IL-1β, IL-6 and IL-18 secretion levels. (I) Determination of LDH release using an LDH release assay kit. (J) Spectrophotometry analysis of caspase-1 activity. (K) Representative images of Hoechst/PI staining and ROS production. Data are represented as mean ± SD. ns, statistically insignificant, *P<0.05, **P<0.01, ***P<0.001, ****P<0.0001. Scale bar, 20 μm. n=3. NLRP3, NLR family pyrin domain-containing protein 3; ox-LDL, oxidized low-density lipoprotein; HUVECs, human umbilical vascular endothelial cells; HO-1, heme oxygenase-1; ROS, reactive oxygen species; si, small interfering; ASC, apoptosis-associated speck-like protein containing CARD; GSDMD-N, N-terminal gasdermin-D; IL, interleukin; LDH, lactate dehydrogenase; ROS, reactive oxygen species EA, eburicoic acid.

(Fig. 5A and C). In contrast, it increased the nuclear and total Nrf2 levels in a dose- and time-dependent manner (Fig 5B, D-H), indicating that eburicoic acid could promote Nrf2 nuclear translocation. To further verify the role of Nrf2 in the anti-pyroptosis activities of eburicoic acid, cells were transfected with Nrf2 siRNA to reduce its expression. The results showed that Nrf2 siRNA transduction decreased the protein levels of Nrf2 by 69%. Importantly, eburicoic acid-induced HO-1 enhancement, ROS clearance, anti-inflammation and anti-pyroptosis effects were mainly compromised after Nrf2 silence (Fig. 6), demonstrating that eburicoic acid inhibits inflammation and pyroptosis in HUVECs via the Keap1/Nrf2/HO-1/ROS pathway.

Eburicoic acid mitigates the development of atherosclerotic plaques in vivo. At last, the present study explored the effects of eburicoic acid on the development of atherosclerotic plaques in HFD-fed apoE$^{-/-}$ mice. Mice were orally gavaged with 10 mg/kg eburicoic acid (dissolved in 0.5% CMV) or vehicle once daily. The results showed that compared with the control group, the serum levels of ALT, AST, BUN and serum creatinine (Scr) were not changed in mice of the eburicoic acid group, suggesting that eburicoic acid displays no apparent hepatotoxicity and nephrotoxicity (Fig. 7A-C). In addition, eburicoic acid administration increased the protein levels of Nrf2 and HO-1and decreased the protein levels of Keap1 and pyroptosis-related factors (NLRP3,

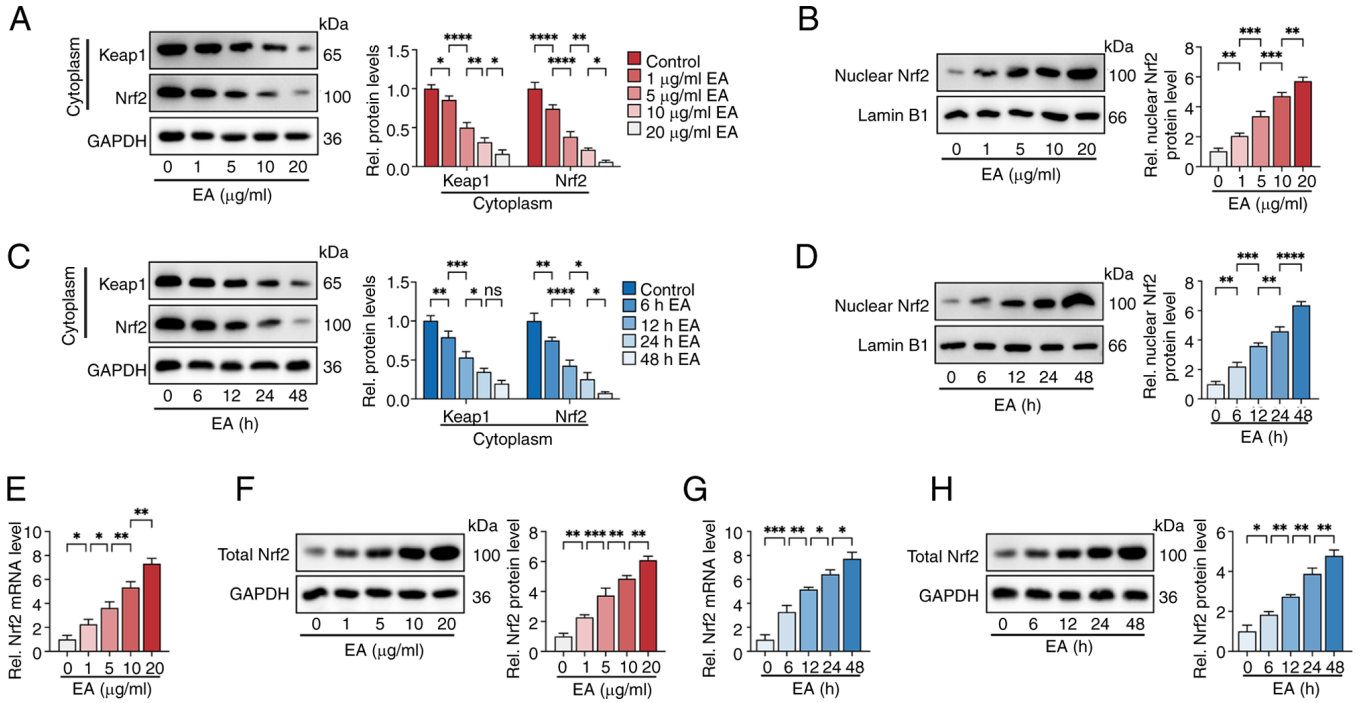

Figure 5. Eburicoic acid promotes Nrf2 nuclear translocation in ox-LDL-treated HUVECs. HUVECs were pre-treated with 100 μg/ml ox-LDL for 24 h. (A and B) Cells were incubated with 1, 5, 10 and 20 μg/ml eburicoic acid for 24 h. The protein levels of cytoplasmic Keap1 and Nrf2 and nuclear Nrf2 were detected using western blotting. (C and D) Cells were incubated with 10 μg/ml eburicoic acid for 6, 12, 24 and 48 h, respectively. The protein levels of cytoplasmic Keap1 and Nrf2 and nuclear Nrf2 were detected using western blotting. (E-H) Cells were incubated with various doses of eburicoic acid for 24 h or 10 μg/ml eburicoic acid for various durations. The mRNA and protein levels of total Nrf2 were detected using RT-qPCR and western blotting, respectively. Data are represented as mean ± SD. ns, statistically insignificant, *P<0.05, **P<0.01, ***P<0.001, ****P<0.0001. Scale bar, 20 μm. n=3. Nrf2, NF-E2-related factor 2; ox-LDL, oxidized low-density lipoprotein; HUVECs, human umbilical vascular endothelial cells; Keap1, Kelch-like ECH-associated protein 1; RT-qPCR, reverse transcription-quantitative PCR EA, eburicoic acid.

cleaved caspase-1, ASC and GSDMD-N) in the aortas (Fig. 7D). Furthermore, eburicoic acid treatment increased HDL-C levels and downregulated TC, LDL-C, TG and pro-inflammatory cytokines (IL-1β, IL-6, TNF-α and IL-18) levels in the serum (Fig. 7E and F). Oil Red O, HE and Masson staining showed eburicoic acid alleviated lipid accumulation, decreased lesion area and increased collagen fiber content in atherosclerotic plaques (Fig. 7G). These findings suggested that eburicoic acid retarded the progression of AS in HFD-fed apoE$^{-/-}$ mice.

Discussion

The present study, for the first time to the best of the authors' knowledge, discovered that eburicoic acid inhibited the activation of NLRP3 inflammasome activation, improved plasma integrity, reduced pro-inflammatory cytokine secretion and suppressed pyroptosis in HUVECs. Mechanistically speaking, eburicoic acid facilitated the disassociation of Nrf2 from Keap1 and promoted Nrf2 nuclear translocation. Activation of the Nrf2/HO-1 pathway-induced ROS reduction served as the upstream signal for upregulating the expression of pyroptosis-related indicators and secretion of pro-inflammatory cytokines. Finally, the present study determined that eburicoic acid mitigated the lipid accumulation in atherosclerotic plaques, increased plaque stability and inhibited inflammatory response in apoE$^{-/-}$ mice.

Chinese herbal medicines and their natural extracts markedly affect inflammation and pyroptosis in VECs through various mechanisms (33,34). Tongxinluo (TXL), one of the most common traditional Chinese medicines, could decrease ROS generation, caspase-1 activity and pro-inflammatory cytokines secretion, exerting anti-pyroptosis effects in mouse aortic endothelial cells (26). Moreover, treatment of HFD-fed apoE$^{-/-}$ mice with TXL suppresses caspase-1 activation in plaque endothelium, decreases the expression of pyroptosis-related factors in the aorta and diminishes atherosclerotic plaque size dose-dependently (26). Salvianolic acid A (SAA) can protect the HUVECs against high glucose-induced pyroptosis in a pyruvate kinase M2 (PKM2)/protein kinase R-dependent manner. Administering SAA to HFD-fed apoE$^{-/-}$ mice markedly decreases the expression of pyroptosis-related factors, including NLRP3, ASC and GSDMD in the endothelium of the aortic sinus, alleviates plaque lipid accumulation and increases fibrous content (35). Isoliquiritigenin can inhibit NLRP3 inflammasome activation, inflammation and pyroptosis in TNF-α-treated HUVECs via the TNF receptor 1/sirtuin 6 (SIRT6) pathway (36). Treatment of human coronary artery endothelial cells with Zhilong Huoxue Tongyu capsule markedly increases cell viability, decreases the expression of pyroptosis-related genes, including NLRP3, ASC and caspase 1, inhibits IL-1β and IL-18 secretion and alleviates pyroptosis through the miR-30b-5p/NLRP3 pathway (37). Lycopene can protect endothelial progenitor cells from ox-LDL-induced damage, downregulate the expression level of pyroptosis indicators and production of inflammatory factors, suppressing pyroptosis through the AMPK/mTOR pathway (38). As a multi-functional bioactive triterpenoid of *Antrodia cinnamomea*, eburicoic acid can decrease oxidative injury and inflammation

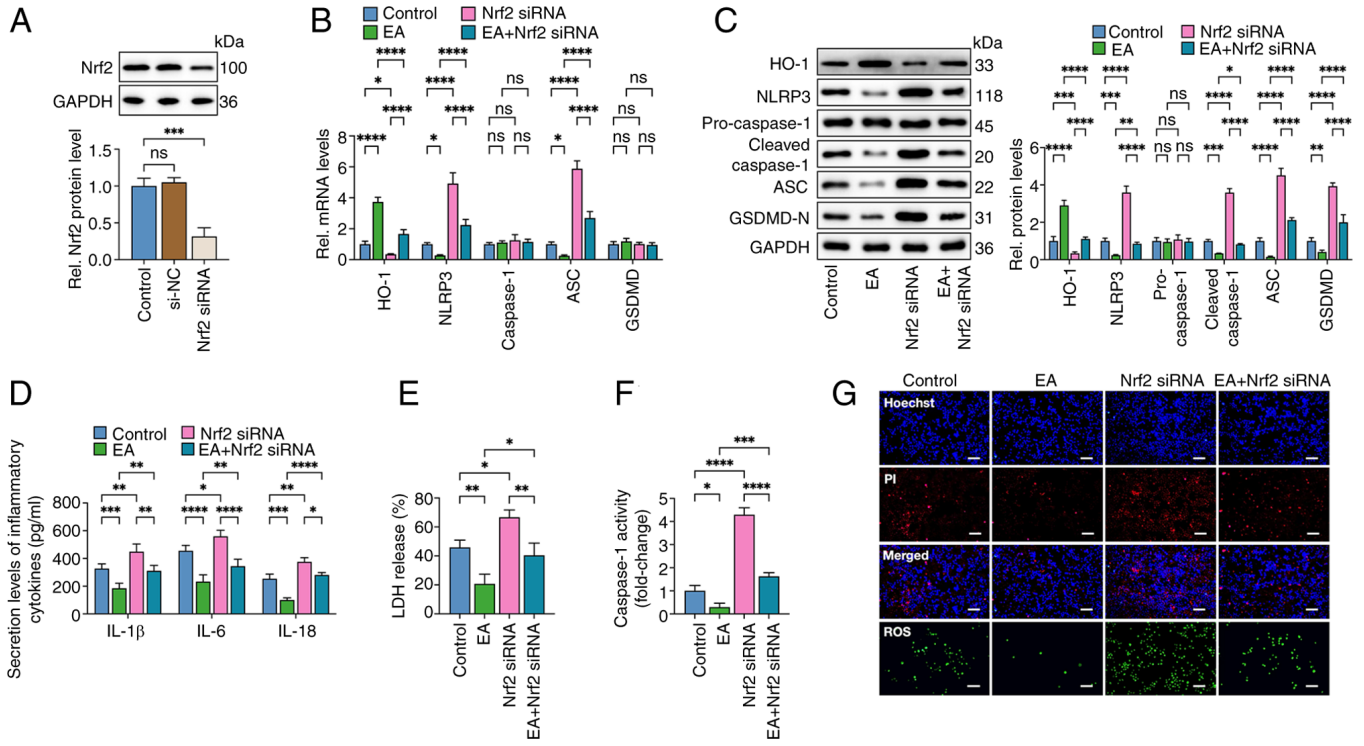

Figure 6. Eburicoic acid inhibits NLRP3 inflammasome activation and pyroptosis in ox-LDL-treated HUVECs via the Nrf2/HO-1/ROS pathway. (A) Cells were transfected with Nrf2 siRNA or scrambled control siRNA for 48 h. western blotting was used to detect the Nrf2 protein level. (B-G) Cells were pre-treated with 100 μg/ml ox-LDL for 24 h. Then, they were transfected with Nrf2 siRNA for 48 h before treatment with 10 μg/ml eburicoic acid for 24 h. (B) RT-qPCR analyses of HO-1, NLRP3, caspase-1, ASC and GSDMD mRNA levels; (C) western blotting analyses of NLRP3, pro-caspase-1, cleaved caspase-1, ASC and GSDMD-N protein levels; (D) ELISA Analyses of IL-1β, IL-6 and IL-18 secretion levels; (E) Determination of LDH release using an LDH release assay kit; (F) Spectrophotometry analysis of caspase-1 activity; (G) Representative images of Hoechst/PI staining and ROS production. Data are represented as mean ± SD. ns, statistically insignificant, *P<0.05, **P<0.01, ***P<0.001, ****P<0.0001. Scale bar, 20 μm. n=3. NLRP3, NLR family pyrin domain-containing protein 3; ox-LDL, oxidized low-density lipoprotein; HUVECs, human umbilical vascular endothelial cells; Nrf2, NF-E2-related factor 2; HO-1, heme oxygenase-1; ROS, reactive oxygen species; si, small interfering; ASC, apoptosis-associated speck-like protein containing CARD; GSDMD-N, N-terminal gasdermin-D; LDH, lactate dehydrogenase; ROS, reactive oxygen species; RT-qPCR, reverse transcription-quantitative PCR EA, eburicoic acid.

in various cell types. Saba *et al* (39) reported that acetyl eburicoic acid decreases NO production and the expression of iNOS, IL-1β, IL-6 and TNF-α in LPS-treated RAW264.7 macrophages dose-dependently. Wang *et al* (40) found that eburicoic acid can directly inhibit the H^+/K^+-ATPase and attenuate ethanol and aspirin-induced gastric ulcers specifically by inhibiting gastric acid. They inferred that the gastric-protecting effects of eburicoic acid may be related to the reduction of antioxidant-dependent mechanisms and inhibition of the inflammatory process. Notably, Lin *et al* (41) treated streptozotocin -induced diabetic mice with eburicoic acid and found that the plasma TG, TC and glucose levels are markedly reduced, demonstrating the anti-hyperlipidemic and anti-diabetic activities of eburicoic acid. The present study observed that incubation of HUVECs with eburicoic acid markedly decreased the expression of NLRP3, ASC, cleaved caspase-1 and GSDMD-N, reduced caspase-1 activity, LDH release and secretion of IL-1β, IL-6 and IL-18 and improved plasma integrity in a dose- and time-dependent manner. These effects of eburicoic acid on HUVECs were mainly compromised by adding ROS inducer DMNQ, demonstrating that eburicoic acid suppressed NLRP3 inflammasome activation and HUVEC pyroptosis by decreasing ROS content. In HFD-fed apoE$^{-/-}$ mice, eburicoic acid diminished the serum levels of IL-1β, IL-6 and TNF-α, improved plasma lipid profile and decreased the expression of pyroptosis-associated factors in aortic tissue, leading to smaller plaque size, less lipid deposition and more fibrous content in the cross-section of aortic roots, which was consistent with the previous studies.

In addition to inflammation, the massive deposition of macrophage-derived foam cells in blood walls is another feature of AS (42). Jin *et al* (43) found that incubation of ox-LDL-laden bone marrow-derived macrophages with VX-765, a specific caspase-1 inhibitor, can suppress pyroptosis and inhibit foam cell formation, suggesting a positive relationship between pyroptosis and lipid accumulation in macrophages. Whether eburicoic acid prevents foam cell formation by inhibiting macrophage pyroptosis needs further investigation.

The Nrf2/HO-1 signaling pathway is indispensable in oxidative stress response, anti-inflammation and antioxidation. Extracts from herbal medicines exert endothelium-protective action via activation of the Nrf2/HO-1 pathway (44). Dihydromyricetin can inhibit palmitic acid-induced NLRP3 inflammasome activation and pyroptosis in HUVECs by activating the Nrf2/HO-1/NQO1 pathway and decreasing mitochondrial ROS production (45). Fisetin can increase HO-1 expression dose- and time-dependently by activating Nrf2, PKC-δ and p38, conferring cytoprotection in H_2O_2-treated HUVECs (46). Astragaloside IV can activate the Nrf2/HO-1 pathway, decrease ROS content, downregulate TNF-α and IL-6 levels and improve oxidative damage in HUVECs with ox-LDL

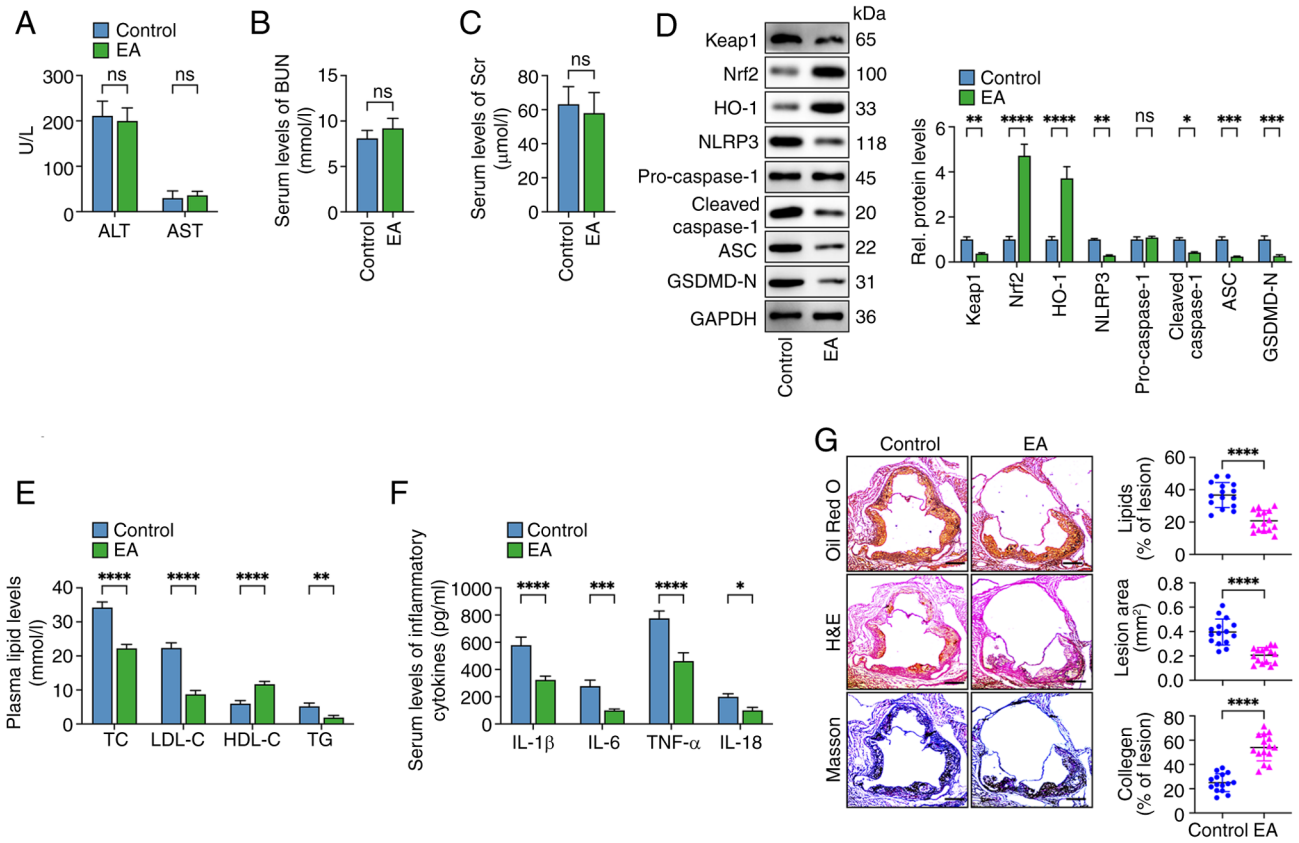

Figure 7. Eburicoic acid mitigates the progression of atherosclerotic plaques in HFD-fed apoE$^{-/-}$ mice. apoE$^{-/-}$ mice (n=15/each group) fed on an HFD were administered with 10 mg/kg eburicoic acid (dissolved in 0.5% CMV) or vehicle only by oral gavage once daily. (A-C) The AST, ALT, BUN and Scr levels were detected using the respective commercial kits; (D) western blotting analyses of Keap1, Nrf2, HO-1, NLRP3, cleaved caspase-1, ASC and GSDMD-N protein levels in the aorta; n=3. (E) Assessment of plasma TC, TG, HDL-C and LDL-C levels; n=3. (F) Determination of serum IL-1β, IL-6, TNF-α and IL-18 levels using ELISA assay; n=3. (G) Oil Red O, HE and Masson staining of cross-sections of the aortic root. Image Pro software analyzed the lipid accumulation, lesion area and collagen content within atherosclerotic plaques. n=15. Data are represented as mean ± SD. ns, statistically insignificant, *P<0.05, **P<0.01, ***P<0.001, ****P<0.0001. Scale bar, 100 μm. HFD, high-fat-diet; AST, aspartate aminotransferase; ALT, alanine aminotransferase; BUN, blood urea nitrogen; Scr, serum creatinine; Keap1, Kelch-like ECH-associated protein 1; Nrf2, NF-E2-related factor 2; HO-1, heme oxygenase-1; NLRP3, NLR family pyrin domain-containing protein 3; TC, total cholesterol; TG, triglycerides; HDL-C high-density lipoprotein cholesterol LDL-C, low-density lipoprotein cholesterol IL, interleukin; EA, eburicoic acid.

intervention (47). Ginsenoside Rg1 can markedly antagonize $PM_{2.5}$-induced HUVEC cell death, ROS accumulation and MDA production by promoting Nrf2 nuclear translocation and HO-1 expression (48). Andrographolide can suppress TNF-α-induced ICAM-1 expression and ROS generation by increasing NADPH oxidase by stimulating the PI3K/Akt/Nrf2/HO-1 pathway in eburicoic acid.hy926 endothelial-like cells (49). The present study found that incubating HUVECs with eburicoic acid increased HO-1 expression in a dose- and time-dependent manner. Silencing of HO-1 mainly compromised eburicoic acid-induced inhibition of ROS accumulation, NLRP3 inflammasome activation, inflammation and pyroptosis in HUVECs. Furthermore, eburicoic acid markedly promoted the dissociation of Nrf2 from the Keap1-Nrf2 complex and subsequent nuclear translocation. Nrf2 knockdown markedly reversed HO-1 enhancement, ROS reduction and pyroptosis suppression induced by eburicoic acid, demonstrating that eburicoic acid alleviates HUVEC pyroptosis via the Keap1/Nrf2/HO-1/ROS pathway. Kong *et al* (50) reported that TLR4, a transmembrane protein, is an upstream positive regulator of the Keap1/NRF2 pathway. The present study found that treating HUVECs with eburicoic acid markedly increased the TLR4 protein level, suggesting that eburicoic acid may activate the Keap1/Nrf2 pathway by stimulating TLR4. Previous studies have shown that miRNAs are critical regulators of Keap1/Nrf2 pathway and pyroptosis. Yao *et al* (51) found that Ginsenoside Rd could ameliorate neuronal pyroptosis and protect against cerebral ischemia/reperfusion injury by upregulating miR-139-5p, inhibiting FoxO1 expression and activating the Keap1/Nrf2/ROS pathway. Xu *et al* (52) found that platelet-rich plasma can attenuate intervertebral disc degeneration by delivering miR-141-3p into the nucleus pulposus cells. Specifically, miR-141-3p can target Keap1 3'UTR, which decreases Keap1 expression and, in turn, promotes nuclear translocation of Nrf2, inhibiting oxidative stress and pyroptosis of nucleus pulposus cells. Whether miRNAs, such as miR-139-5p and miR-141-3p, are involved in the effects of eburicoic acid on Keap1/Nrf2 pathway and pyroptosis in HUVECs warrants further exploration.

In summary, the present study identified the anti-atherogenic role of eburicoic acid and its relationship with endothelial pyroptosis. Specifically, eburicoic acid can decrease Keap1 expression and promote Nrf2 nuclear translocation, which in turn increases HO-1 expression and represses ROS accumulation and VEC pyroptosis, ultimately alleviating

hyperlipidemia, inflammation and the development of atheromatous plaques *in vivo*. Eburicoic acid may be regarded as an effective phytomedicine for preventing AS.

Acknowledgements

Not applicable.

Funding

The present study was supported by the Anhui Provincial Natural Science Foundation (grant no. 2008085MH239).

Availability of data and materials

The data generated in the present study may be requested from the corresponding author.

Authors' contributions

XHL and MQM conceived and designed the experiments. MQM, CY, SYJ, YY and YYP performed experiments and analyzed data. MQM, YY and XHL wrote and revised the manuscript. MQM and YYP confirm the authenticity of all the raw data. All authors have read and approved the final version of the manuscript.

Ethics approval and consent to participate

All animal experiments were approved by the Anhui Medical University Ethics Committee (approval no. LLSC20242407).

Patient consent for publication

Not applicable.

Competing interests

The authors declare that they have no competing interests.

References

1. Dibben GO, Faulkner J, Oldridge N, Rees K, Thompson DR, Zwisler AD and Taylor RS: Exercise-based cardiac rehabilitation for coronary heart disease: A meta-analysis. Eur Heart J 44: 452-469, 2023.
2. Pan H, Ho SE, Xue C, Cui J, Johanson QS, Sachs N, Ross LS, Li F, Solomon RA, Connolly ES Jr, *et al*: Atherosclerosis is a smooth muscle Cell-Driven Tumor-like disease. Circulation 149: 1885-1898, 2024.
3. Xing Y and Lin X: Challenges and advances in the management of inflammation in atherosclerosis. J Adv Res: Jun 21, 2024 doi: 10.1016/j.jare.2024.06.016.
4. Jia M, Li Q, Guo J, Shi W, Zhu L, Huang Y, Li Y, Wang L, Ma S, Zhuang T, *et al*: Deletion of BACH1 attenuates atherosclerosis by reducing endothelial inflammation. Circ Res 130: 1038-1055, 2022.
5. Wang Q, Han J, Liang Z, Geng X, Du Y, Zhou J, Yao W and Xu T: FSH is responsible for androgen deprivation Therapy-associated atherosclerosis in mice by exaggerating endothelial inflammation and monocyte adhesion. Arterioscler Thromb Vasc Biol 44: 698-719, 2024.
6. Oladapo A, Jackson T, Menolascino J and Periyasamy P: Role of pyroptosis in the pathogenesis of various neurological diseases. Brain Behav Immun 117: 428-446, 2024.
7. Volchuk A, Ye A, Chi L, Steinberg BE and Goldenberg NM: Indirect regulation of HMGB1 release by gasdermin D. Nat Commun 11: 4561, 2020.
8. Gimbrone MA Jr and García-Cardeña G: Endothelial cell dysfunction and the pathobiology of atherosclerosis. Circ Res 118: 620-636, 2016.
9. Yin Y, Li X, Sha X, Xi H, Li YF, Shao Y, Mai J, Virtue A, Lopez-Pastrana J, Meng S, *et al*: Early hyperlipidemia promotes endothelial activation via a caspase-1-sirtuin 1 pathway. Arterioscler Thromb Vasc Biol 35: 804-816, 2015.
10. Lv Y, Jiang Z, Zhou W, Yang H, Jin G, Wang D, Kong C, Qian Z, Gu Y, Chen S and Zhu L: Low-shear stress promotes atherosclerosis via inducing endothelial cell pyroptosis mediated by IKKε/STAT1/NLRP3 pathway. Inflammation 47: 1053-1066, 2024.
11. Chen Y, Yuan C, Qin W, Yu B, Wei D and Wu P: TMAO promotes vascular endothelial cell pyroptosis via the LPEAT-mitophagy pathway. Biochem Biophys Res Commun 703: 149667, 2024.
12. Song L, Zhang J, Lai R, Li Q, Ju J and Xu H: Chinese herbal medicines and active metabolites: Potential antioxidant treatments for atherosclerosis. Front Pharmacol 12: 675999, 2021.
13. Jing Y, Hu T, Yuan J, Liu Z, Tao M, Ou M, Cheng X, Cheng W, Yi Y and Xiong Q: Resveratrol protects against postmenopausal atherosclerosis progression through reducing PCSK9 expression via the regulation of the ERα-mediated signaling pathway. Biochem Pharmacol 211: 115541, 2023.
14. Gao S, Zhang W, Zhao Q, Zhou J, Wu Y, Liu Y, Yuan Z and Wang L: Curcumin ameliorates atherosclerosis in apolipoprotein E deficient asthmatic mice by regulating the balance of Th2/Treg cells. Phytomedicine 52: 129-135, 2019.
15. Xing SS, Yang J, Li WJ, Li J, Chen L, Yang YT, Lei X, Li J, Wang K and Liu X: Salidroside decreases atherosclerosis plaque formation via inhibiting endothelial cell pyroptosis. Inflammation 43: 433-440, 2020.
16. Cao H, Jia Q, Yan L, Chen C, Xing S and Shen D: Quercetin suppresses the progression of atherosclerosis by regulating MST1-Mediated autophagy in ox-LDL-Induced RAW264.7 macrophage foam cells. Int J Mol Sci 20: 6093, 2019.
17. Ma SR, Tong Q, Lin Y, Pan LB, Fu J, Peng R, Zhang XF, Zhao ZX, Li Y, Yu JB, *et al*: Berberine treats atherosclerosis via a vitamine-like effect down-regulating Choline-TMA-TMAO production pathway in gut microbiota. Signal Transduct Target Ther 7: 207, 2022.
18. Deng JS, Huang SS, Lin TH, Lee MM, Kuo CC, Sung PJ, Hou WC, Huang GJ and Kuo YH: Analgesic and anti-inflammatory bioactivities of eburicoic acid and dehydroeburicoic acid isolated from *Antrodia camphorata* on the inflammatory mediator expression in mice. J Agric Food Chem 61: 5064-5071, 2013.
19. Tung YT, Tsai TC, Kuo YH, Yen CC, Sun JY, Chang WH, Chen HL and Chen CM: Comparison of solid-state-cultured and wood-cultured *Antrodia camphorata* in anti-inflammatory effects using NF-κB/luciferase inducible transgenic mice. Phytomedicine 21: 1708-1716, 2014.
20. Su YC, Liu CT, Chu YL, Raghu R, Kuo YH and Sheen LY: Eburicoic acid, an active triterpenoid from the fruiting bodies of basswood cultivated antrodia cinnamomea, induces ER Stress-mediated autophagy in human hepatoma cells. J Tradit Complement Med 2: 312-322, 2012.
21. Huang GJ, Deng JS, Huang SS, Lee CY, Hou WC, Wang SY, Sung PJ and Kuo YH: Hepatoprotective effects of eburicoic acid and dehydroeburicoic acid from *Antrodia camphorata* in a mouse model of acute hepatic injury. Food Chem 141: 3020-3027, 2013.
22. Wang J, Zhang P, He H, Se X, Sun W, Chen B, Zhang L, Yan X and Zou K: Eburicoic acid from Laetiporus sulphureus (Bull.:Fr.) Murrill attenuates inflammatory responses through inhibiting LPS-induced activation of PI3K/Akt/mTOR/NF-κB pathways in RAW264.7 cells. Naunyn Schmiedebergs Arch Pharmacol 390: 845-856, 2017.
23. Lin CH, Kuo YH and Shih CC: Eburicoic acid, a triterpenoid compound from *Antrodia camphorata*, displays antidiabetic and antihyperlipidemic effects in Palmitate-treated C2C12 myotubes and in High-Fat Diet-Fed mice. Int J Mol Sci 18: 2314, 2017.
24. Livak KJ and Schmittgen TD: Analysis of relative gene expression data using real-time quantitative PCR and the 2(-Delta Delta C(T)) method. Methods 25: 402-408, 2001.
25. Andrews CS, Matsuyama S, Lee BC and Li JD: Resveratrol suppresses NTHi-induced inflammation via up-regulation of the negative regulator MyD88 short. Sci Rep 6: 34445, 2016.
26. Jiang X, Ma C, Gao Y, Zheng Y, Li J, Zong W and Zhang Q: Tongxinluo attenuates atherosclerosis by inhibiting ROS/NLRP3/caspase-1-mediated endothelial cell pyroptosis. J Ethnopharmacol 304: 116011, 2023.

27. Zhou Y, Zhang Y, Wang H, Zhang X, Chen Y and Chen G: Microglial pyroptosis in hippocampus mediates Sevolfurane-induced cognitive impairment in aged mice via ROS-NLRP3 inflammasome pathway. Int Immunopharmacol 116: 109725, 2023.
28. Luo P, Liu D, Zhang Q, Yang F, Wong YK, Xia F, Zhang J, Chen J, Tian Y, Yang C, *et al*: Celastrol induces ferroptosis in activated HSCs to ameliorate hepatic fibrosis via targeting peroxiredoxins and HO-1. Acta Pharm Sin B 12: 2300-2314, 2022.
29. Yang W, Wang Y, Zhang C, Huang Y, Yu J, Shi L, Zhang P, Yin Y, Li R and Tao K: Maresin1 protect against ferroptosis-induced liver injury through ROS inhibition and Nrf2/HO-1/GPX4 activation. Front Pharmacol 13: 865689, 2022.
30. Hong H, Lou S, Zheng F, Gao H, Wang N, Tian S, Huang G and Zhao H: Hydnocarpin D attenuates lipopolysaccharide-induced acute lung injury via MAPK/NF-κB and Keap1/Nrf2/HO-1 pathway. Phytomedicine 101: 154143, 2022.
31. Chen H, Fu J, Chen H, Hu Y, Soroka DN, Prigge JR, Schmidt EE, Yan F, Major MB, Chen X and Sang S: Ginger compound [6]-shogaol and its cysteine-conjugated metabolite (M2) activate Nrf2 in colon epithelial cells in vitro and in vivo. Chem Res Toxicol 27: 1575-1585, 2014.
32. Luo RR, Yang J, Sun YL, Zhou BY, Zhou SX, Zhang GX and Yang AX: Dexmedetomidine attenuates ferroptosis by Keap1-Nrf2/HO-1 pathway in LPS-induced acute kidney injury. Naunyn Schmiedebergs Arch Pharmacol 397: 7785-7796, 2024.
33. Yan Q, Li P, Liu S, Sun Y, Chen C, Long J, Lin Y, Liang J, Wang H, Zhang L, *et al*: Dihydromyricetin treats pulmonary hypertension by modulating CKLF1/CCR5 axis-induced pulmonary vascular cell pyroptosis. Biomed Pharmacother 180: 117614, 2024.
34. Wang Y, Guan X, Gao CL, Ruan W, Zhao S, Kai G, Li F and Pang T: Medioresinol as a novel PGC-1α activator prevents pyroptosis of endothelial cells in ischemic stroke through PPARα-GOT1 axis. Pharmacol Res 169: 105640, 2021.
35. Zhu J, Chen H, Le Y, Guo J, Liu Z, Dou X and Lu D: Salvianolic acid A regulates pyroptosis of endothelial cells via directly targeting PKM2 and ameliorates diabetic atherosclerosis. Front Pharmacol 13: 1009229, 2022.
36. He J, Deng Y, Ren L, Jin Z, Yang J, Yao F, Liu Y, Zheng Z, Chen D, Wang B, *et al*: Isoliquiritigenin from licorice flavonoids attenuates NLRP3-mediated pyroptosis by SIRT6 in vascular endothelial cells. J Ethnopharmacol 303: 115952, 2023.
37. Liu M, Luo G, Liu T, Yang T, Wang R, Ren W, Liu P, Lai X, Zhou H and Yang S: Zhilong huoxue tongyu capsule alleviated the pyroptosis of vascular endothelial cells induced by ox-LDL through miR-30b-5p/NLRP3. Evid Based Complement Alternat Med 2022: 3981350, 2022.
38. Tan C, Chen J, Tu T, Chen L and Zou J: Lycopene inhibits pyroptosis of endothelial progenitor cells induced by ox-LDL through the AMPK/mTOR/NLRP3 pathway. Open Med (Wars) 19: 20240973, 2024.
39. Saba E, Son Y, Jeon BR, Kim SE, Lee IK, Yun BS and Rhee MH: Acetyl eburicoic acid from laetiporus sulphureus var. miniatus suppresses inflammation in murine macrophage RAW 264.7 cells. Mycobiology 43: 131-136, 2015.
40. Wang J, Sun W, Luo H, He H, Deng W, Zou K, Liu C, Song J and Huang W: Protective effect of eburicoic acid of the chicken of the woods mushroom, laetiporus sulphureus (Higher Basidiomycetes), against gastric ulcers in mice. Int J Med Mushrooms 17: 619-626, 2015.
41. Lin CH, Kuo YH and Shih CC: Antidiabetic and hypolipidemic activities of eburicoic acid, a triterpenoid compound from *Antrodia camphorata*, by regulation of Akt phosphorylation, gluconeogenesis, and PPARα in streptozotocin-induced diabetic mice. RSC Adv 8: 20462-20476, 2018.
42. La Chica Lhoëst MT, Martinez A, Claudi L, Garcia E, Benitez-Amaro A, Polishchuk A, Piñero J, Vilades D, Guerra JM, Sanz F, *et al*: Mechanisms modulating foam cell formation in the arterial intima: Exploring new therapeutic opportunities in atherosclerosis. Front Cardiovasc Med 11: 1381520, 2024.
43. Jin Y, Liu Y, Xu L, Xiong Y, Peng Y, Ding K, Zheng S, Yang N, Zhang Z, Li L, *et al*: Novel role for caspase 1 inhibitor VX765 in suppressing NLRP3 inflammasome assembly and atherosclerosis via promoting mitophagy and efferocytosis. Cell Death Dis 13: 512, 2022.
44. Zhang Q, Liu J, Duan H, Li R, Peng W and Wu C: Activation of Nrf2/HO-1 signaling: An important molecular mechanism of herbal medicine in the treatment of atherosclerosis via the protection of vascular endothelial cells from oxidative stress. J Adv Res 34: 43-63, 2021.
45. Hu Q, Zhang T, Yi L, Zhou X and Mi M: Dihydromyricetin inhibits NLRP3 inflammasome-dependent pyroptosis by activating the Nrf2 signaling pathway in vascular endothelial cells. Biofactors 44: 123-136, 2018.
46. Lee SE, Jeong SI, Yang H, Park CS, Jin YH and Park YS: Fisetin induces Nrf2-mediated HO-1 expression through PKC-δ and p38 in human umbilical vein endothelial cells. J Cell Biochem 112: 2352-2360, 2011.
47. Zhu Z, Li J and Zhang X: Astragaloside IV protects against oxidized Low-density lipoprotein (ox-LDL)-induced endothelial cell injury by reducing oxidative stress and inflammation. Med Sci Monit 25: 2132-2140, 2019.
48. Li CP, Qin G, Shi RZ, Zhang MS and Lv JY: Ginsenoside Rg1 reduces toxicity of PM(2.5) on human umbilical vein endothelial cells by upregulating intracellular antioxidative state. Environ Toxicol Pharmacol 35: 21-29, 2013.
49. Lu CY, Yang YC, Li CC, Liu KL, Lii CK and Chen HW: Andrographolide inhibits TNFα-induced ICAM-1 expression via suppression of NADPH oxidase activation and induction of HO-1 and GCLM expression through the PI3K/Akt/Nrf2 and PI3K/Akt/AP-1 pathways in human endothelial cells. Biochemical Pharmacology 91: 40-50, 2014.
50. Kong C, Yan X, Zhu Y, Zhu H, Luo Y, Liu P, Ferrandon S, Kalady MF, Gao R, He J, *et al*: Fusobacterium nucleatum promotes the development of colorectal cancer by activating a cytochrome P450/Epoxyoctadecenoic acid axis via TLR4/Keap1/NRF2 signaling. Cancer Res 81: 4485-4498, 2021.
51. Yao Y, Hu S, Zhang C, Zhou Q, Wang H, Yang Y, Liu C and Ding H: Ginsenoside Rd attenuates cerebral ischemia/reperfusion injury by exerting an anti-pyroptotic effect via the miR-139-5p/FoxO1/Keap1/Nrf2 axis. Int Immunopharmacol 105: 108582, 2022.
52. Xu J, Xie G, Yang W, Wang W, Zuo Z and Wang W: Platelet-rich plasma attenuates intervertebral disc degeneration via delivering miR-141-3p-containing exosomes. Cell Cycle 20: 1487-1499, 2021.